INTERNATIONAL JOURNAL FOR NUMERICAL METHODS IN FLUIDS, VOL. 11, 303–316 (1990)

DIFFUSION FLAME ANALYSIS OF AN AFTERBURNER AS A FUNCTION OF THE AIR–FUEL RATIO

SHU-HAO CHUANG AND JIUNN-SHEAN JIANG

Department of Mechanical Engineering, National Chung-Hsing University, Taichung, Taiwan 40227, R.O.C.

SUMMARY

The diffusion flame of an afterburner as a function of the air–fuel ratio is analysed by employing the SIMPLE-C algorithm and the turbulence k–ε model. In the present analysis, better combustion efficiency of an afterburner with a slightly fuel-lean mixture is shown. The velocity, fuel mass fraction, temperature and combustion efficiency distributions of reacting flow in an afterburner with two V-gutter flameholders as a function of the air–fuel ratio are also discussed and compared. The calculated results in the present analysis can be applied to the fundamental study of reacting flow in an afterburner.

KEY WORDS Afterburner SIMPLE-C algorithm Air–fuel ratio

INTRODUCTION

The flames of combustors can be stabilized by recirculation zones,[1–5] which can be created by fluids flowing around a bluff-body or along a discontinuous boundary surface.[6] V-gutter flameholders are often utilized in gas turbine combustors and afterburners and in ramjet engines for flame stabilization purposes. The computational combustion flow of an afterburner with a flameholder consisting of a solid triangular bluff-body (cone) has been used.[7] In the present analysis the flameholder is considered as two open-mouth-type V-gutters instead of a solid cone in order to simulate practical afterburner flow.

Previous work on the simulation of combustor flow fields utilized the stream function–vorticity method (φ–ω) and the k–ε two-equation turbulence model to analyse a two-dimensional combustor.[8] There have also been studies of combustor flow using p–u–v primitive variables and the k–ε turbulence model.[6,9–16] The process incorporated the SIMPLE algorithm technique initiated by Patankar.[17] The SIMPLE-C (SIMPLE-consistent) algorithm developed by van Doormaal and Raithby[18] and Latimer and Pollard[19] has a better convergence rate of residual mass[20] than that of the SIMPLE algorithm. Statistical approaches that use a probability density function (PDF) to describe the combustor were developed by Serag-Eldin and Spalding.[21] The above studies were limited to cold flow except for that of Zhang and Chiu.[7] A study of the computational combustion model with a flameholder was made by Zhang and Chiu,[7] who used the eddy break-up combustion model and group combustion theory. Other researchers[22,23] investigated reacting flow in coaxial and side-dump combustors. However, these studies were limited to reacting flow in a dump combustor and did not consider combustion flow in an afterburner.[24] The intention here is to investigate the phenomena of reacting flow in an afterburner with two V-gutter flameholders as a function of the air–fuel ratio.

0271–2091/90/110303–14$07.00

Received January 1989
Revised December 1989

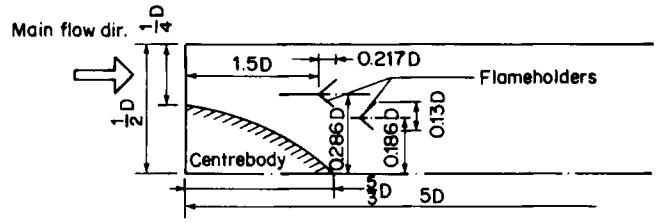

Figure 1. Basic configuration of an afterburner

The geometry of the afterburner configuration considered in this paper is shown in Figure 1. The present calculations are performed using the well known SIMPLE-C algorithm and power-law scheme.

THEORETICAL ANALYSIS AND TURBULENT COMBUSTION MODEL

The reacting flow analysis of an afterburner is very complicated.[25] In order to simplify the problem and thus facilitate the numerical analysis, we make the following assumptions.

1. The flow is two-dimensional axisymmetric and steady state.
2. Radiation and gravity effects are negligible.
3. The flow field is composed of a single-phase gaseous flow, i.e. we do not consider a two-phase flow problem.
4. The wall thickness of the V-gutters is infinitely thin.
5. The chemical reaction is one-step and has an infinitely fast reaction rate.
6. The effect of density fluctuations is negligible.
7. The Lewis number is equal to unity and the specific heat at constant pressure is a constant.

The general form of the Favre-averaged equation for the steady axisymmetric turbulence flow can be written as

$$\underbrace{\frac{1}{r}\left[\frac{\partial}{\partial x}(\rho u r\phi)+\frac{\partial}{\partial r}(\rho v r\phi)\right]}_{\text{convection term}}-\underbrace{\frac{\partial}{\partial x}\left(r\Gamma_\phi\frac{\partial\phi}{\partial x}\right)-\frac{\partial}{\partial r}\left(r\Gamma_\phi\frac{\partial\phi}{\partial r}\right)}_{\text{diffusion term}}=S^\phi, \tag{1}$$

where ϕ stands for any dependent variable: u, v, k, ε, m_{fo}, m_{fu} or $\tilde{h}$. Γ_ϕ is the appropriate turbulence transport coefficient for ϕ. S^ϕ is the source term of the transport equation for ϕ, as shown in Table I. The total effective viscosity μ_e of the flow field is

$$\mu_e=\mu_l+\mu_t, \tag{2}$$

where μ_l and μ_t represent the molecular and eddy viscosity respectively and μ_t is known from the k–ε turbulence model[26] as

$$\mu_t=C_\mu\rho k^2/\varepsilon. \tag{3}$$

In the present analysis, CH_4 is used as the fuel and thus the chemical reaction equation can be written as

$$CH_4+2(O_2+3{\cdot}76N_2)\xrightarrow{\omega}CO_2+2H_2O+7{\cdot}52N_2+\Delta H_{fu}$$

Table I. Governing equation variables

ϕ	Γ_ϕ	$S^{\phi *}$
u	μ_e	$-\frac{\partial P}{\partial r}+\frac{\partial}{\partial x}\left(\mu_e\frac{\partial u}{\partial x}\right)+\frac{1}{r}\frac{\partial}{\partial r}\left(r\mu_e\frac{\partial v}{\partial x}\right)$
v	μ_e	$-\frac{\partial P}{\partial r}-\frac{1}{r}\left(\frac{2\mu_e v}{r}\right)+\frac{\partial}{\partial x}\left(\mu_e\frac{\partial u}{\partial r}\right)+\frac{1}{r}\frac{\partial}{\partial r}\left(r\mu_e\frac{\partial v}{\partial r}\right)$
k	μ_e/σ_k	$\mu_e\left\{2\left[\left(\frac{\partial u}{\partial x}\right)^2+\left(\frac{\partial v}{\partial r}\right)^2+\left(\frac{v}{r}\right)^2\right]+\left(\frac{\partial u}{\partial r}+\frac{\partial v}{\partial x}\right)^2\right\}-\rho\varepsilon$
ε	μ_e/σ_ε	$\frac{C_1\varepsilon}{k}\mu_e\left\{2\left[\left(\frac{\partial u}{\partial x}\right)^2+\left(\frac{\partial v}{\partial r}\right)^2+\left(\frac{v}{r}\right)^2\right]+\left(\frac{\partial u}{\partial r}+\frac{\partial v}{\partial x}\right)^2\right\}-\frac{C_2\rho\varepsilon^2}{k}$
m_{fo}	μ_e/σ_{fo}	0
m_{fu}	μ_e/σ_{fu}	m'_{fu}
$\tilde{h}$	μ_e/σ_h	0

C_1	C_2	C_μ	σ_k	σ_ε	σ_{fo}	σ_{fu}	σ_h
1·44	1·92	0·09	1·0	1·3	0·9	0·9	0·7

* The terms $-\frac{2}{3}\rho k$ is the source terms are omitted here in order to simplify the problem and thus facilitate the numerical analysis. The source terms that contain the div v condition are also neglected.

or

$$(1\text{ kg})\text{ fuel}+(s\text{ kg})\text{ oxidant}+(a\text{ kg})N_2\xrightarrow{\omega}[(1+s)\text{ kg}]\text{ products}+(a\text{ kg})N_2+\Delta H_{fu}. \tag{4}$$

The assumption of an infinitely fast chemical reaction rate (i.e. $\omega\to\infty$) implies that fuel and oxidant will not coexist at the same time. Therefore the following relations exist in the flow field:

$$m_{fu}+m_{air}+m_{pr}=1,$$

$$\begin{aligned} &m_{fu}=0, \quad m_{ox}=0 && \text{when } m_{fo}=0,\\ &m_{fu}=0, \quad m_{ox}=m_{fo} && \text{when } m_{fo}>0,\\ &m_{ox}=0, \quad m_{fu}=-(1/s)m_{fo} && \text{when } m_{fo}<0, \end{aligned}$$

where

$$m_{fo}=m_{ox}-sm_{fu}.$$

The species conservation equations of fuel and oxidant are

$$\frac{\partial}{\partial x}(\rho u m_{fu})+\frac{1}{r}\frac{\partial}{\partial r}(\rho v r m_{fu})-\frac{\partial}{\partial x}\left(\frac{\mu_e}{\sigma_{fu}}\frac{\partial m_{fu}}{\partial x}\right)-\frac{1}{r}\frac{\partial}{\partial r}\left(r\frac{\mu_e}{\sigma_{fu}}\frac{\partial m_{fu}}{\partial r}\right)=m'_{fu}, \tag{5}$$

$$\frac{\partial}{\partial x}(\rho u m_{ox})+\frac{1}{r}\frac{\partial}{\partial r}(\rho v r m_{ox})-\frac{\partial}{\partial x}\left(\frac{\mu_e}{\sigma_{ox}}\frac{\partial m_{ox}}{\partial x}\right)-\frac{1}{r}\frac{\partial}{\partial r}\left(r\frac{\mu_e}{\sigma_{ox}}\frac{\partial m_{ox}}{\partial r}\right)=m'_{ox}. \tag{6}$$

Subtracting equation (6) multiplied by s from equation (5), we can obtain the species equation of

modified mass fraction m_{fo} as

$$\frac{\partial}{\partial x}(\rho u m_{fo})+\frac{1}{r}\frac{\partial}{\partial r}(\rho v r m_{fo})-\frac{\partial}{\partial x}\left(\frac{\mu_e}{\sigma_{fo}}\frac{\partial m_{fo}}{\partial x}\right)-\frac{1}{r}\frac{\partial}{\partial r}\left(r\frac{\mu_e}{\sigma_{fo}}\frac{\partial m_{fo}}{\partial r}\right)=0, \tag{7}$$

and the energy (total enthalpy) equation is

$$\frac{\partial}{\partial x}(\rho u\tilde{h})+\frac{1}{r}\frac{\partial}{\partial r}(\rho v r\tilde{h})-\frac{\partial}{\partial x}\left(\frac{\mu_e}{\sigma_{fu}}\frac{\partial \tilde{h}}{\partial x}\right)-\frac{1}{r}\frac{\partial}{\partial r}\left(r\frac{\mu_e}{\sigma_{fu}}\frac{\partial \tilde{h}}{\partial r}\right)=0. \tag{8}$$

The density of the reacting flow can be modelled by an equation of state as follows:

$$\rho=\frac{P/\bar{R}T}{m_{fu}/w_{fu}+m_{ox}/w_{ox}+m_{pr}/w_{pr}}, \tag{9}$$

where

$$T=(\tilde{h}-m_{fu}\Delta H_{fu})/C_{Pmix}, \tag{10}$$

$$C_{Pmix}=\sum_j m_j C_{Pj}. \tag{11}$$

NUMERICAL ANALYSIS AND BOUNDARY CONDITIONS

Grids system and irregular boundary

The staggered grid arrangement of integration over control volumes and the calculation domain (60 × 22) are shown in Figure 2. Staggered steps of ladder type are utilized to simulate the irregular boundary and V-gutter as shown in Figure 3.

Finite difference equations

Integration over control volumes and the numerical process of the SIMPLE-C[18,19] algorithm along with the power-law scheme are employed to perform the present calculations. The general form of finite difference equations for equation (1) with a linearized source term are given as follows.

Finite difference equation of the axial momentum

$$(a_E-S_P^u)u_E=\sum a_{nb}u_{nb}+S_C^u+(P_P-P_E)A_E. \tag{12}$$

Finite difference equation of the radial momentum

$$(a_N-S_P^v)v_N=\sum a_{nb}v_{nb}+S_C^v+(P_P-P_N)A_N. \tag{13}$$

Finite difference equations of the other variables

$$(a_P-S_P^\phi)\phi_P=\sum a_{nb}\phi_{nb}+S_P^\phi. \tag{14}$$

Solution technique

The numerical process of the SIMPLE-C algorithm was employed to solve the present problem. The SIMPLE-C method is an enhancement of the SIMPLE method that was developed by Patankar.[17] The distinction between SIMPLE and SIMPLE-C is in the handling of the pressure

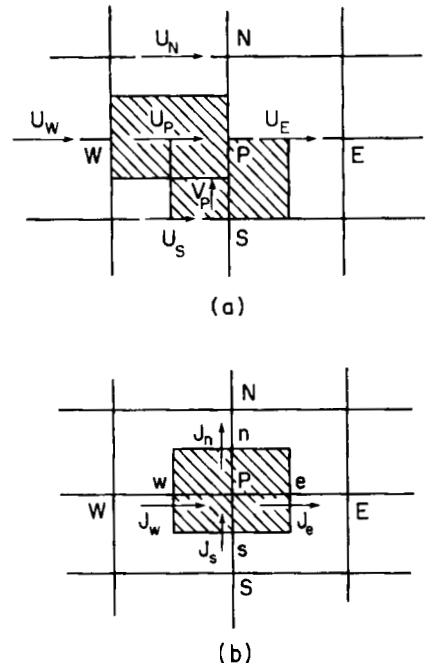

Figure 2. Control volumes and staggered grid arrangement: (a) for variables u, v; (b) for other variables ϕ except u, v

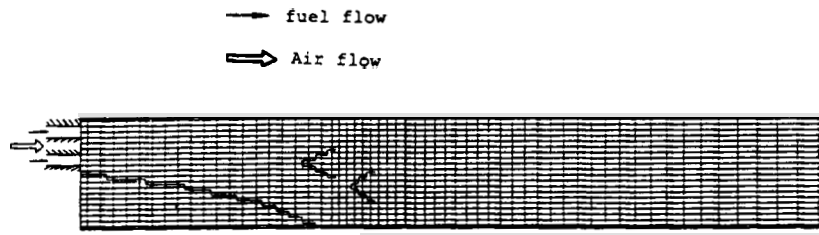

Figure 3. Spacing of grids and ladder-type arrangement of centre-body and V-gutter

Table II. Underrelaxation factors f

ϕ	u	v	k	ε	P'	μ_t	m_{fo}	ρ	$\tilde{h}$
f	0·3	0·3	0·5	0·5	0·3	0·3	0·3	0·1	0·8

and velocity correction terms.[18,19] Details of the calculation procedure of SIMPLE-C algorithm will not be repeated here. The TDMA and line-by-line method was swept alternately in the x- and r-direction. Underrelaxation factors were used for each iteration process to help the convergence of the calculations. The values of the underrelaxation factors are listed in Table II.

The residual of any variable ϕ is defined as

$$R_P^{\phi} = a_P \phi_P - \sum_{i=N,S,W,E} |a_i \phi_i - S^{\phi}|. \tag{15}$$

The residual of any flow variable ϕ approaches zero when the calculation of the flow field approaches convergence.

Boundary conditions

Inlet. According to the data of Lilley and Rhode,[27] the turbulence kinetic energy and dissipation rate are

$$k_{in} = \alpha u_{in}^2 \quad (\text{where } \alpha = 0{\cdot}003), \tag{16}$$

$$\varepsilon_{in} = C_{\mu} k_{in}^{3/2} / 0{\cdot}03R. \tag{17}$$

The inlet velocity of the fuel injection was determined by the air–fuel mass ratio, and

$$m_{fo} = 1, \quad m_{fu} = 0, \quad m_{ox} = 1 \quad \text{in the region of the air inlet,} \tag{18}$$

$$m_{fo} = -s, \quad m_{fu} = 1, \quad m_{ox} = 0 \quad \text{in the region of the fuel injection.} \tag{19}$$

Centreline

$$\partial\phi/\partial r = 0 \quad (\text{due to symmetry}). \tag{20}$$

Wall

$$u = 0, \quad v = 0 \quad (\text{no-slip condition}). \tag{21}$$

Both k and ε were handled by wall functions[26] and an adiabatic boundary in the wall was assumed.

Outlet

$$\partial\phi/\partial x = 0 \quad (\text{fully developed flow}). \tag{22}$$

RESULTS AND DISCUSSION

The physical phenomena of reacting flow in an afterburner as a function of the air–fuel ratio $A/F = 15{\cdot}00$, $17{\cdot}24$ and $18{\cdot}50$—where $A/F = 15{\cdot}00$ is a fuel-rich ratio, $A/F = 17{\cdot}24$ is the stoichiometric fuel ratio and $A/F = 18{\cdot}50$ is a fuel-lean ratio for the present problem—are as follows.

The effects of A/F on the velocity field

The velocity vectors for $A/F = 15{\cdot}00$, $17{\cdot}24$ and $18{\cdot}50$ are shown in Figures 4–6 respectively. The streamlines of the flow field for $A/F = 15{\cdot}00$, $17{\cdot}24$ and $18{\cdot}50$ are shown in Figures 7–9 respectively. The recirculation zone patterns behind the two V-gutter flameholders are slightly dependent on A/F. This result is due to the fact that the fuel velocity changes when A/F changes from a fuel-rich to a fuel-lean ratio.

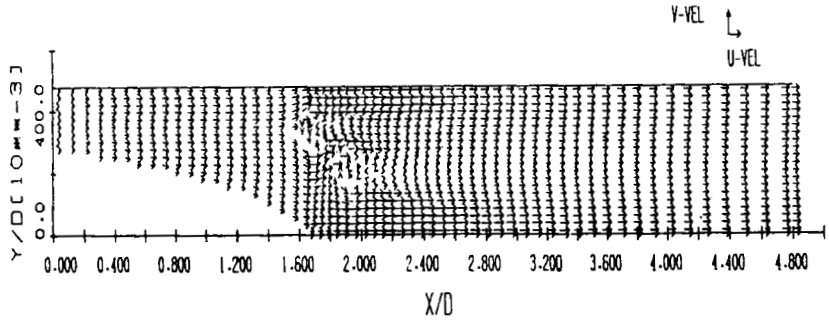

Figure 4. Flow patterns ($A/F = 15{\cdot}00$)

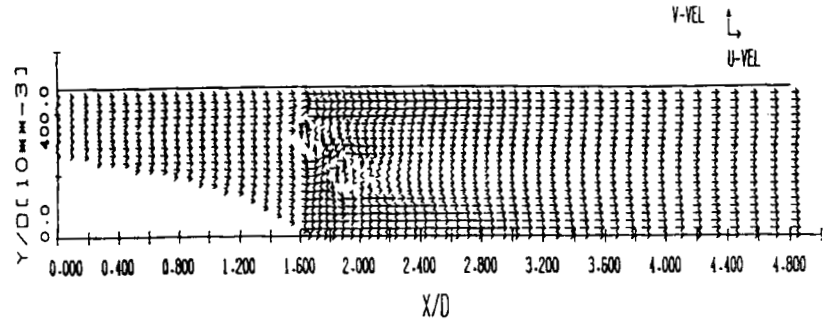

Figure 5. Flow patterns ($A/F = 17{\cdot}24$)

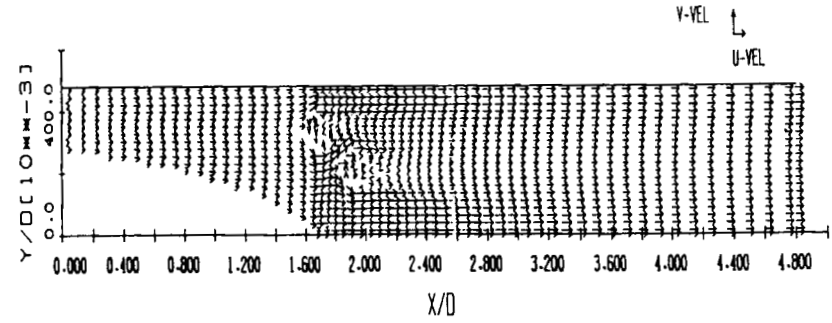

Figure 6. Flow patterns ($A/F = 18{\cdot}50$)

The effects of A/F on the fuel mass fraction distribution

The fuel mass fraction distributions for $A/F = 15{\cdot}00$, $17{\cdot}24$ and $18{\cdot}50$ are shown in Figures 10–12 respectively. The fuel mass fraction distribution existed until $X/D = 2{\cdot}8$ for $A/F = 15{\cdot}00$, as shown in Figure 10. The fuel was almost completely reacted at $X/D = 1{\cdot}6$ for $A/F = 18{\cdot}50$. From Figures 10–12 we find that the area of the fuel distribution is the smallest for $A/F = 18{\cdot}50$. This

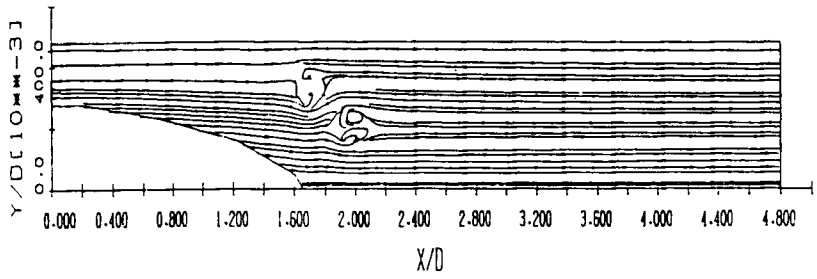

Figure 7. Streamlines ($A/F = 15{\cdot}00$)

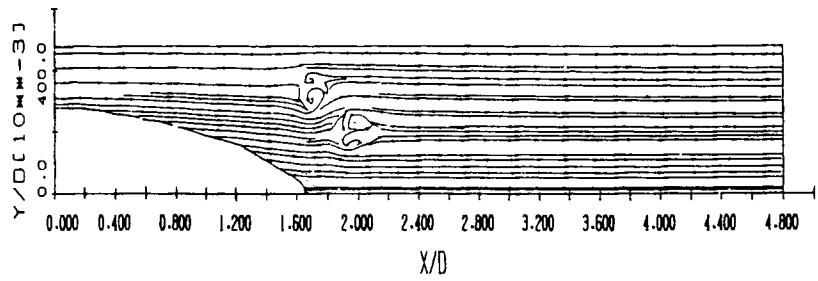

Figure 8. Streamlines ($A/F = 17{\cdot}24$)

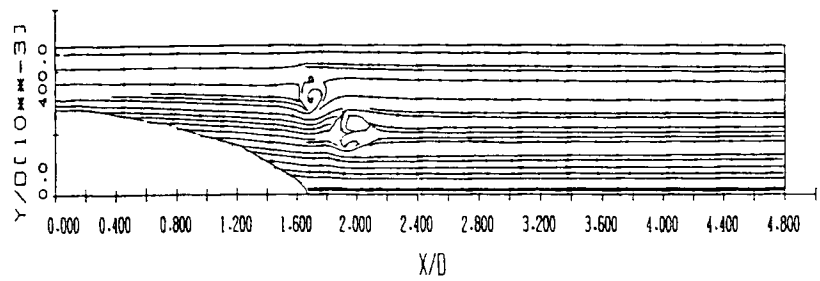

Figure 9. Streamlines ($A/F = 18{\cdot}50$)

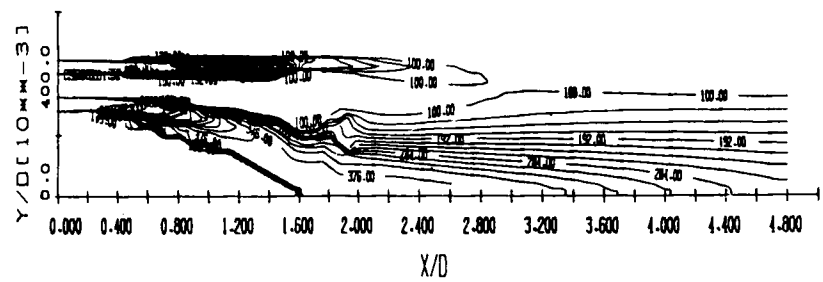

Figure 10. Fuel mass fraction distribution ($\times 10^{-3}$) ($A/F = 15{\cdot}00$)

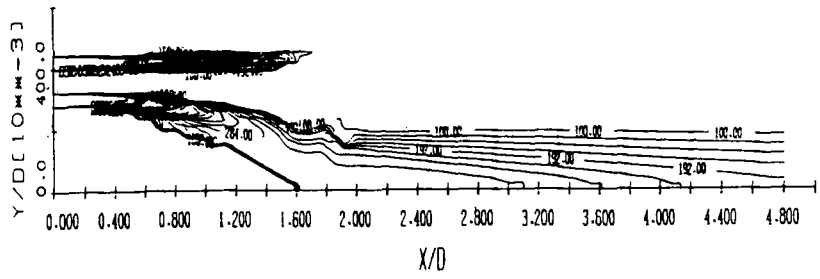

Figure 11. Fuel mass fraction distribution ($\times 10^{-3}$) ($A/F = 17{\cdot}24$)

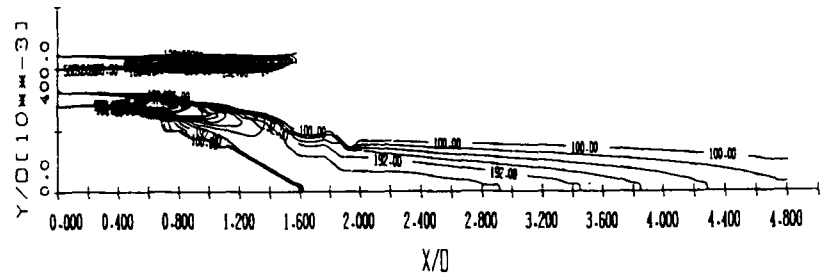

Figure 12. Fuel mass fraction distribution ($\times 10^{-3}$) ($A/F = 18{\cdot}50$)

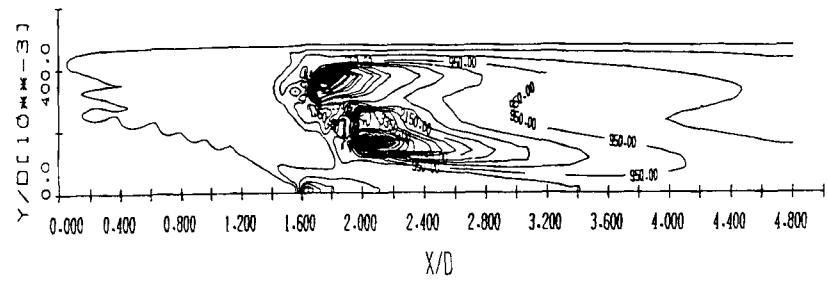

Figure 13. Turbulence kinetic energy distribution ($A/F = 15{\cdot}00$)

phenomenon demonstrates that better turbulence mixing and combustion of an afterburner with two V-gutter flameholders occur under slightly fuel-lean conditions.

The effects of A/F on the temperature and turbulence kinetic energy distribution

In the present analysis the combustion model is of the diffusion flame type. Therefore complete combustion and high temperatures appear in the diffusion surface between fuel and air. The high-temperature zone near the upper wall expands toward the centreline when A/F is in the fuel-lean condition (i.e. $A/F = 18{\cdot}50$); this is due to the better mixing effect that exists in the fuel-lean condition (see Figures 16–18). The turbulence kinetic energy distributions for $A/F = 15{\cdot}00$, $17{\cdot}24$

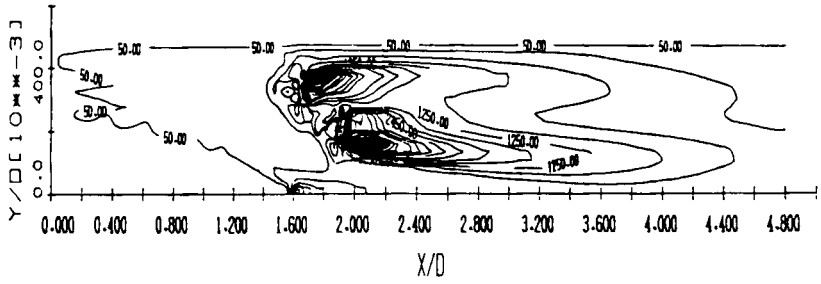

Figure 14. Turbulence kinetic energy distribution ($A/F = 17{\cdot}24$)

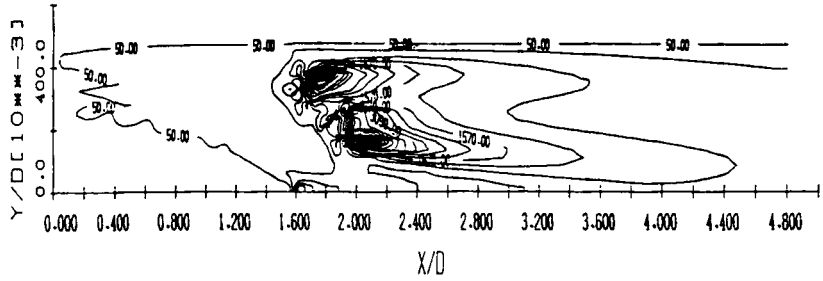

Figure 15. Turbulence kinetic energy distribution ($A/F = 18{\cdot}50$)

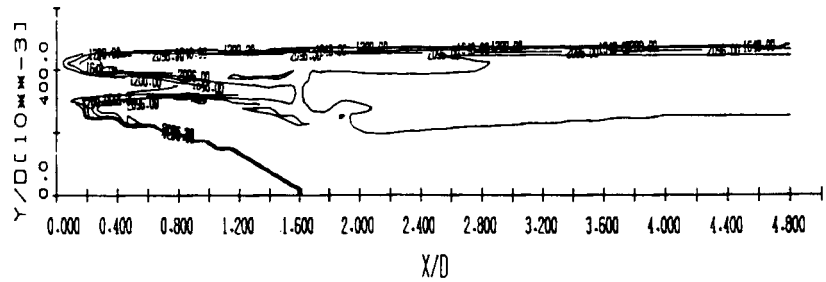

Figure 16. Temperature (K) distribution ($A/F = 15{\cdot}00$)

and 18·50 are shown in Figures 13–15 respectively. The turbulence kinetic energy of the reacting flow is higher than that of the cold flow,[24] and the high turbulence kinetic energy is slightly expanded downstream in the fuel-lean condition. This is due to the fact that the greater velocity difference between air and fuel causes better turbulence mixing when A/F is increased, as shown in Figures 13–15 and 16–18.

The effects of A/F on the average temperature and combustion efficiency

The average temperatures as a function of the axial location for $A/F = 15{\cdot}00$, 17·24 and 18·50 are shown in Figure 19. The average temperature is highest when $A/F = 15{\cdot}00$ because more fuel reacts with air in the fuel-rich condition. In the present simulation analysis the best combustion

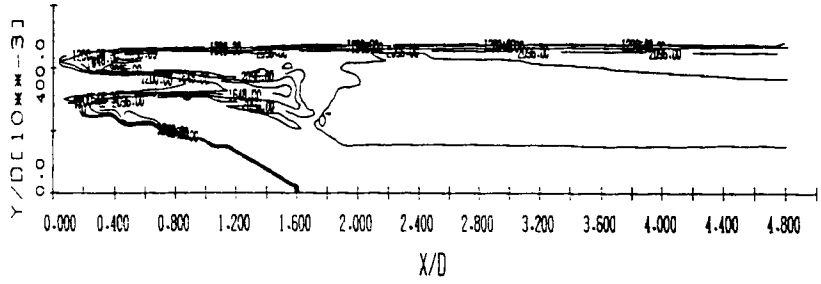

Figure 17. Temperature (K) distribution ($A/F = 17{\cdot}24$)

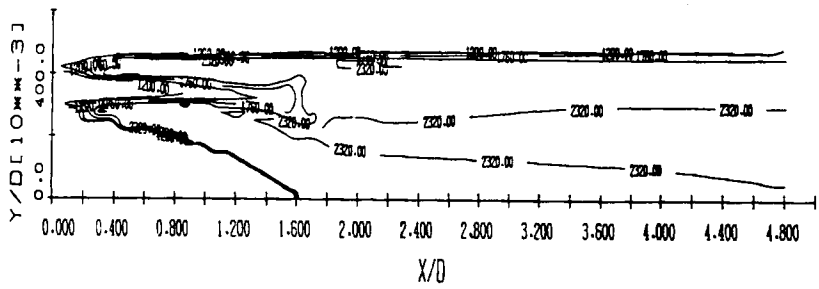

Figure 18. Temperature (K) distribution ($A/F = 18{\cdot}50$)

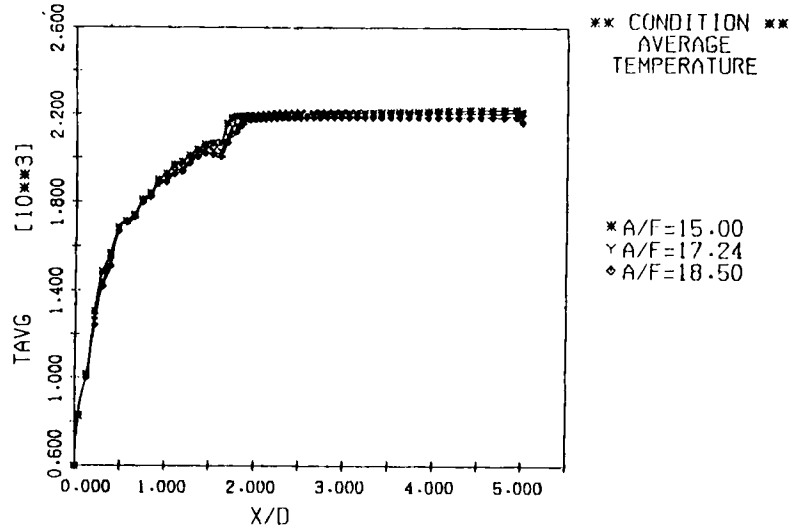

Figure 19. Average temperature along the afterburner as a function of A/F

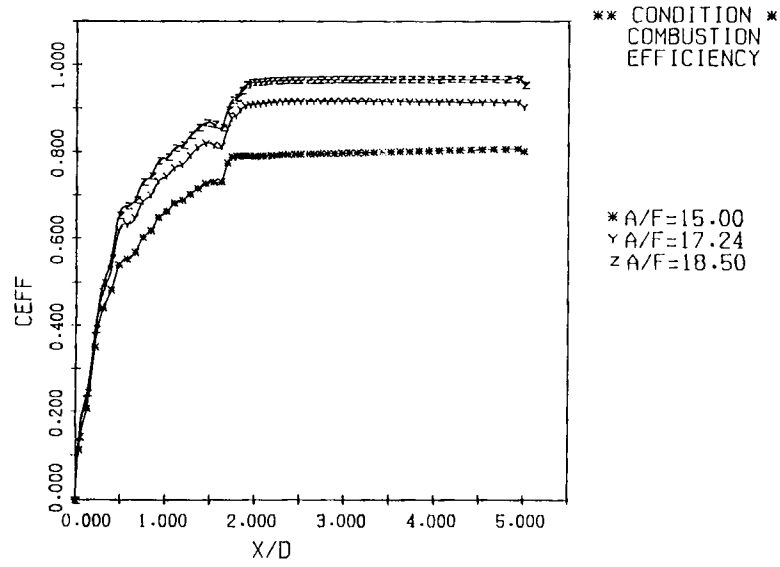

Figure 20. Combustion efficiency of the afterburner as a function of A/F

efficiency exists in the fuel-lean condition, as shown in Figure 20, for the present combustion model. For the diffusion flame type, the calculated results are consistent with the present combustion model (the assumption of an infinitely fast chemical reaction rate). Finite chemical reaction rates should be considered in order to further understand fuel consumption, intermediate products, flame stability, etc. A better combustion model with a finite chemical reaction rate, such as the eddy break-up model of Spalding,[28,29] is more sensitive to turbulence mixing and might be used to further study the problem considered.

CONCLUDING REMARKS

1. Better combustion efficiency of an afterburner with two V-gutter flameholders is obtained in a slightly fuel-lean condition.
2. The average flow temperature along the combustor decreases when the air–fuel ratio is increased.
3. Both turbulence kinetic energy and mixing effects are promoted when the air–fuel ratio is increased.
4. The turbulence mixing between fuel and air is more homogeneous and the combustion of fuel is more complete when the air–fuel ratio is increased.
5. The effects of the air–fuel ratio on the flow field are almost negligible.

APPENDIX: NOMENCLATURE

A_i	surface area of cell
a_i	coefficient
A/F	air–fuel ratio
C_P	specific heat at constant pressure

f	underrelaxation factor
ΔH_{fu}	heat of reaction per unit mass of fuel
h	static enthalpy
$\tilde{h}$	total enthalpy ($\equiv C_p T + \frac{1}{2}(u^2+v^2) + m_{fu}\Delta H_{fu}$)
k	turbulence kinetic energy
m_{air}, m'_{air}	mass fraction and reaction rate of air
m_{fu}, m'_{fu}	mass fraction and reaction rate of fuel
m_{fo}	modified mass fraction ($=m_{ox}-sm_{fu}$)
m_{ox}	mass fraction of oxidant
P	static pressure
P_o	total pressure
P'	correction pressure
$\bar{R}$	Universal gas constant
R_P^ϕ	residue of variable ϕ at point P
S	stoichiometric ratio ($=m_{ox}/m_{fu}$)
S^ϕ	source term of variable ϕ
S_P^ϕ, S_C^ϕ	coefficients of linearized source term
T	temperature
u, v	velocities in the axial and radial directions
V	volume
w	molecular weight
x, r	co-ordinates in the axial and radial directions
Γ_ϕ	transport coefficient of variable ϕ
ε	dissipation rate of turbulence kinetic energy
μ_e	effective viscosity
μ_l	molecular viscosity
μ_t	eddy viscosity
ρ	fluid density
ϕ	transport variable
ω	chemical reaction rate

Superscripts and subscripts

()′	corrected quantities
in	inlet property
P, N, E, S, W	grid points
nb	neighbourhood points

REFERENCES

1. T. Carmody, 'Establishment of the wake behind a disk', *J. Basic Eng.*, **4**, 869–882 (1964).
2. G. Winterfeld, 'On processes of turbulent exchange behind flameholders', *10th Symp. (Int.) on Combustion*, 1965, pp. 1265–1275.
3. A. H. Lefebvre, A. R. A. F. Ibrahim and N. C. Benson, 'Factors affecting fresh mixture entrainment in bluff-body stabilized flames', *Combust. Flame*, **10**, 231–239 (1966).
4. N. A. Chigier and J. L. Gilbert, 'Recirculation eddies in the wake of flameholders', *J. Inst. Fuel*, **12**, 105–112 (1968).
5. T. W. Davies and J. M. Beer, 'Flow in the wake of bluff-body flame stabilizers', *13th Symp. (Int.) on Combustion*, 1971, pp. 631–638.
6. G. H. Vatistas, S. Lin, C. K. Kwok and D. G. Lilley, 'Bluff-body flameholder wakes: a simple numerical solution, *AIAA Paper 82-1177*, 1982.
7. X. C. Zhang and H. H. Chiu, 'Computational combustion model of thrust augmentor for airbreathing engines', *AIAA Paper 85-0087*, 1985.

8. D. G. Lilley, 'Flowfield modeling in practical combustors: a review', *J. Energy*, **3**, 193–210 (1979).
9. S. V. Patankar, 'Numerical prediction of three-dimensional flows', in B. E. Launder (ed.), *Studies in Convection*, Academic Press, London, 1975, pp. 1–78.
10. E. E. Khalil, D. B. Spalding and L. H. Whitelaw, 'The calculation of local flow properties in two dimensional furnaces', *Int. J. Heat Mass Transfer*, **18**, 775–791 (1975).
11. D. G. Lilley, 'Primitive pressure–velocity code for the computation of strongly swirling flow', *AIAA J.*, **14**, 749–756 (1976).
12. R. B. Edelman, P. T. Harsha and S. N. Schmotolocha, 'Modeling technique for the analysis of ramjet combustion processes', *AIAA J.*, **19**, 601–609 (1981).
13. P. T. Harsha and R. B. Edelman, 'Assessment of modular ramjet combustor model', *J. Spacecraft*, **19**, 430–436 (1982).
14. H. M. Jang, 'The flow field analysis of sudden expansion dump combustor of the ramjet engine', *Master Thesis*, Department of Mechanical Engineering National Taiwan University, 1982.
15. Z. C. Hong and H. C. Liao, 'Swirl effects on the structure of recirculation zone and fuel distribution of a coaxial dump combustor', *3rd Natl. Conf. on Mechanical Engineering*, CSME, Chung-Li, 1986, pp. 323–344.
16. K. D. Jen and Y. P. Su, 'Sudden expansion dump combustor flowfield simulation and analysis with V-gutter flameholder', *Trans. AASRC*, **18**, 13–24 (1985).
17. S. V. Patankar, *Numerical Heat Transfer and Fluid Flow*, Hemisphere, New York, 1980.
18. J. P. van Doormaal and G. D. Raithby, 'Enhancements of the SIMPLE method for predicting incompressible fluids flows', *Numer. Heat Transfer*, **7**, 147–163 (1984).
19. B. R. Latimer and A. Pollard, 'Comparison of pressure–velocity coupling solution algorithms', *Numer. Heat Transfer*, **8**, 635–652 (1985).
20. Z. C. Hong and T. H. Ko, 'A study on the flow field in a 3D side-inlet dump combustor with different side-inlet angles', *The 11th Natl Conf. on Theoretical and Applied Mechanics*, Taipei, 1987, pp. 211–223.
21. M. A. Serag-Eldin and D. B. Spalding, 'Computations for three-dimensional gas-turbine combustion chamber flows', *Trans. ASME, J. of Eng. for Power*, **101**, 326–336 (1979).
22. D. R. Kang, 'The flowfield and combustion analysis for the combustor with V-gutter flameholders', *Master Thesis*, Department of Mechanical Engineering, National Taiwan University, 1986.
23. Z. C. Hong, J. L. Pan and C. Lin, 'Side dump combustor combustion analysis', *CSME J.*, **7**, 1–10 (1986).
24. S. H. Chuang and S. W. Li, 'Combustion flowfield analysis of an afterburner with V-gutter flameholders', *Trans. AASRC*, **21**, 39–54 (1988).
25. G. C. Oates, 'The aerothermodynamics of aircraft gas turbine engines', *AFAPL TR78-52*, 1978.
26. B. E. Launder and D. B. Spalding, *Lectures on Mathematical Models of Turbulence*, Academic Press, London, 1972.
27. D. G. Lilley and D. L. Rhode, 'A computer code for swirling turbulent axisymmetric reacting flows in practical isothermal combustor geometries', *NASA Contract Report 3442*, 1982.
28. D. B. Spalding, 'Mixing and chemical reactions in steady confined turbulent flames', *13th Symp. (Int.) on Combustion*, 1971, pp. 649–657.
29. H. B. Mason and D. B. Spalding 'Prediction of reaction rate in turbulent premixed boundary layer flow', *1st Symp. (Eur.) on Combustion*, 1973, pp. 601–606.